Abstract

We give a quantitative analysis for the clusters of octahedral terms which appear in the high resolution rotational spectra of SF_6 for large angular momentum. We derive approximate expressions for the cluster energies and the splittings within each cluster which obviate the diagonalization of the octahedral deformation potential.

Orbital level splitting in octahedral symmetry and SF_6 rotational spectra. II. Quantitative treatment of high J levels

Chris W. Patterson

Los Alamos Scientific Laboratory, Los Alamos, New Mexico

William G. Harter

Joint Institute for Laboratory Astrophysics, Boulder, Colorado 80302
(Received 16 November 1976)

We give a quantitative analysis for the clusters of octahedral terms which appear in the high resolution rotational spectra of SF_6 for large angular momentum. We derive approximate expressions for the cluster energies and the splittings within each cluster which obviate the diagonalization of the octahedral deformation potential.

INTRODUCTION

Recent experiments using tunable semiconductor lasers have revealed for the first time the centrifugal splitting of angular momentum J in sulfur hexafluoride (SF_6).[1,2] The component lines of each J-manifold have been identified according to their symmetry type using a formula of the form[3,4]

$$E = A(J) + B(J)(-1)^{J+1} F^{4\ J\ J}_{A_1\ p\ p} \tag{1}$$

for transition energies accurate to fourth order in J. Thus, for a given branch, the splitting of a J-manifold into irreducible representations (IR)p of O_h may be analyzed once the symmetry-adapted vector coupling coefficients $F^{4\ J\ J}_{A_1\ p\ p}$ are determined. Here A_1 is the scalar representation.

The above experiments have shown the centrifugal splittings of higher and lower energies to occur in clusters of IR of O_h when J is large ($J>20$). Further experiments have resolved these clusters and have shown them to decompose into separate IR terms with very simple splitting ratios.[5]

Numerous authors have evaluated the symmetry-adapted vector coupling coefficients,[6-8] but have failed to account for the occurrence of clusters for large J. Dorney and Watson[9] were the first to notice the clusters which arise from these coefficients and to explain them by making the simple assumption that the angular momentum is quantized about the three- or fourfold symmetry axes of the molecule.

In our previous paper,[10] Article I, we have extended the treatment of Dorney and Watson to give a detailed qualitative physical basis for understanding the occurrence of clusters for large J and the simple splitting ratios within each cluster. It is the purpose of the present paper to put our results on a quantitative footing.

We give approximate first and second order perturbative expressions for the symmetry-adapted vector coupling coefficients which are easily evaluated and which give the cluster's "center of gravity" even for small J ($J<20$).

We also derive more complicated expressions which give the order of magnitude of the term splittings within each cluster along with their proper sign. Such expressions give the ordering of terms within each cluster and indicate when spectroscopic resolution of the individual terms within each cluster is feasible.

CENTER OF GRAVITY OF CLUSTERS

As shown by Moret-Bailly,[11] we may find the $F^{4\ J\ J}_{A_1\ p\ p}$ coefficients by diagonalizing the fourth rank octahedral scalar T_{A_1} in our angular momentum basis. In terms of tensor operators, this scalar is given by

$$T_A = \sqrt{\tfrac{7}{12}}\, V^4_0 + \sqrt{\tfrac{5}{24}}\,(V^4_4 + V^4_{-4}) \tag{2a}$$

along the fourfold symmetry axes, or equivalently by

$$T_A = -\tfrac{2}{3}\left[\sqrt{\tfrac{7}{12}}\, V^4_0 + 2\sqrt{\tfrac{5}{24}}\,(V^4_{-3} - V^4_3)\right] \tag{2b}$$

along the threefold symmetry axes. Note that Eq. (2a) shows explicitly that our scalar operator can only mix angular momentum states $|{}^J_M\rangle$ directed along the fourfold axes which belong to the same IR M_4 of C_4. We use a notation for the IR of C_4 such that M_4 signifies M mod4. Similarly, Eq. (2b) shows explicitly that our scalar operator can only mix angular momentum states $|{}^J_M\rangle$ directed along the threefold axis which belong the same IR M_3 of C_3. Again, M_3 signified M mod3.

Diagonalizing either scalar operator above in our angular momentum basis is equivalent to finding the symmetry adapted vector coupling coefficients

$$F^{4\ J\ J}_{A_1\ p\ p} = \sum_{m,m_1,m_2} \left\langle {4 \atop m} \middle| A_1 \right\rangle \left\langle {J \atop m_1} \middle| {p \atop a_1} \right\rangle \times \left\langle {J \atop m_2} \middle| {p \atop a_2} \right\rangle \begin{pmatrix} 4 & J & J \\ m & m_1 & m_2 \end{pmatrix}, \tag{3}$$

as defined by Moret-Bailly in terms of 3-j coefficients

$$\begin{pmatrix} 4 & J & J \\ m & m_1 & m_2 \end{pmatrix}.$$

The coefficients $\langle {}^J_m | {}^p_a \rangle$ above are just the transformation coefficients between octahedral states $|{}^p_a\rangle$ and angular momentum states $|{}^J_M\rangle$ such that

$$\left|{J \atop M}\right\rangle = \sum_{p,a} \left\langle {p \atop a} \middle| {J \atop M} \right\rangle \left|{p \atop a}\right\rangle. \tag{4}$$

We shall assume that we are dealing with real representations of O_h such that

$$\left\langle {p \atop a} \middle| {J \atop M} \right\rangle = (-1)^M \left\langle {J \atop M} \middle| {p \atop a} \right\rangle. \tag{5}$$

Since T_{A_1} is an octahedral scalar operator, we find

$$\sum_{M_2} \left\langle \begin{matrix} J \\ M_1 \end{matrix} \middle| T_{A_1} \middle| \begin{matrix} J \\ M_2 \end{matrix} \right\rangle \left\langle \begin{matrix} J \\ M_2 \end{matrix} \middle| \begin{matrix} p \\ a \end{matrix} \right\rangle = \left\langle \begin{matrix} p \\ a \end{matrix} \middle| T_{A_1} \middle| \begin{matrix} p \\ a \end{matrix} \right\rangle \left\langle \begin{matrix} J \\ M_1 \end{matrix} \middle| \begin{matrix} p \\ a \end{matrix} \right\rangle. \quad (6)$$

The eigenvalues of the operator T_{A_1} in the angular momentum basis are proportional to the symmetry-adapted vector coupling coefficients. Indeed, using Eq. (5) and the Wigner–Eckart theorem, we find

$$\begin{aligned} \left\langle \begin{matrix} p \\ a \end{matrix} \middle| T_{A_1} \middle| \begin{matrix} p \\ a \end{matrix} \right\rangle &= \sum_{M_1, M_2} \left\langle \begin{matrix} p \\ a \end{matrix} \middle| \begin{matrix} J \\ M_1 \end{matrix} \right\rangle \left\langle \begin{matrix} J \\ M_1 \end{matrix} \middle| T_{A_1} \middle| \begin{matrix} J \\ M_2 \end{matrix} \right\rangle \left\langle \begin{matrix} J \\ M_2 \end{matrix} \middle| \begin{matrix} p \\ a \end{matrix} \right\rangle, \\ &= \sum_{M_1, M_2, M} \left\langle \begin{matrix} p \\ a \end{matrix} \middle| \begin{matrix} J \\ M_1 \end{matrix} \right\rangle \left\langle \begin{matrix} J \\ M_2 \end{matrix} \middle| \begin{matrix} p \\ a \end{matrix} \right\rangle \left\langle \begin{matrix} 4 \\ M \end{matrix} \middle| A_1 \right\rangle \left\langle \begin{matrix} J & 4 & J \\ M_1 & M & M_2 \end{matrix} \right\rangle, \\ &= \sum_{M_1, M_2, M} \left\langle \begin{matrix} J \\ M_1 \end{matrix} \middle| \begin{matrix} p \\ a \end{matrix} \right\rangle \left\langle \begin{matrix} J \\ M_2 \end{matrix} \middle| \begin{matrix} p \\ a \end{matrix} \right\rangle \left\langle \begin{matrix} 4 \\ M \end{matrix} \middle| A_1 \right\rangle (-1)^J \begin{pmatrix} J & 4 & J \\ -M_1 & M & M_2 \end{pmatrix} (J \| 4 \| J), \\ &= (J \| 4 \| J)(-1)^J F^{4\ J\ J}_{A_1\ p\ p}, \end{aligned} \quad (7)$$

where $(J \| 4 \| J)$ is a reduced matrix element. Note that the derivation of Eq. (7) depends on the proper normalization of the scalar operators as given in Eq. (2).

As we have seen, the scalar operator T_{A_1} can only mix angular momentum states $|\begin{smallmatrix} J \\ M \end{smallmatrix})$ with the same IR M_4 of C_4 on the fourfold axis or with the same IR M_3 of C_3 on the threefold axis. Thus we need only to diagonalize T_{A_1} in subsets with the same IR of C_4 or C_3 to find the $F^{4\ J\ J}_{A_1\ p\ p}$ coefficients. However, for large J we have an approximate method of finding these coefficients which can yield theoretical transition energies via Eq. (1) accurate to current spectroscopic resolution without the need for diagonalizing large matrices.

We shall assume that to zeroth order of approximation our octahedral states $|\begin{smallmatrix} p \\ a \end{smallmatrix}\rangle$ are formed from angular momentum states $|\begin{smallmatrix} J \\ M \end{smallmatrix}\rangle$ of definite M directed along the four- or threefold axes. We write our octahedral states as $|\begin{smallmatrix} p \\ a \end{smallmatrix} JM\rangle$ to indicate their angular momentum origins. We shall soon see that our approximation is only valid for large J and M.

The angular momentum states directed along the different fourfold axes form a six dimensional representation of O_h, whereas the angular momentum states directed along the different threefold axes form an eight dimensional representation of O_h. To find the IR of O_h to which these representations decompose it is sufficient to determine the transformational characteristics of the states $|\begin{smallmatrix} J \\ M \end{smallmatrix}\rangle$ under C_4 or C_3 as has been shown in Article I.

We found that along the fourfold axes the states $|\begin{smallmatrix} J \\ M \end{smallmatrix}\rangle$ with IR M_4 of C_4 gave rise to the following terms of O_h:

$$\begin{aligned} &O_4\colon\ A_1 + T_1 + E, \\ &1_4\colon\ T_1 + T_2, \\ &2_4\colon\ A_2 + T_2 + E, \\ &3_4\colon\ T_1 + T_2. \end{aligned} \quad (8a)$$

Similarly, along the threefold axes the states $|\begin{smallmatrix} J \\ M \end{smallmatrix}\rangle$ with IR M_3 of C_3 gave rise to the following terms of O_h:

$$\begin{aligned} &O_3\colon\ A_1 + T_1 + T_2 + A_2, \\ &1_3\colon\ T_1 + E + T_2, \\ &2_3\colon\ T_1 + E + T_2. \end{aligned} \quad (8b)$$

The states $|\begin{smallmatrix} p \\ a \end{smallmatrix} JM)$ thus give rise to six- or eightfold degenerate clusters.

To find the cluster energy or center of gravity before splitting we treat our scalar potential T_{A_1} as a perturbation acting on our zeroth order states $|\begin{smallmatrix} J \\ M \end{smallmatrix})$. To second order we find that the cluster energy is given by

$$T_{JM} = T^1_{JM} + T^2_{JM}, \quad (9)$$

where

$$T^1_{JM} = \left\langle \begin{matrix} J \\ M \end{matrix} \middle| T_{A_1} \middle| \begin{matrix} J \\ M \end{matrix} \right\rangle, \quad (10a)$$

$$T^2_{JM} = \sum_{M'} \frac{\left| \left\langle \begin{matrix} J \\ M' \end{matrix} \middle| T_{A_1} \middle| \begin{matrix} J \\ M \end{matrix} \right\rangle \right|^2}{T^1_{JM} - T^1_{JM'}}, \quad (10b)$$

with the corresponding eigenstates given by

$$\left| \begin{matrix} p \\ a \end{matrix} JM \right\rangle = \left| \begin{matrix} J \\ M \end{matrix} \right\rangle + \sum_{M'} \frac{\left\langle \begin{matrix} J \\ M' \end{matrix} \middle| T_{A_1} \middle| \begin{matrix} J \\ M \end{matrix} \right\rangle}{T^1_{JM} - T^1_{JM'}} \left| \begin{matrix} J \\ M' \end{matrix} \right\rangle. \quad (11)$$

From Eqs. (7), (9), and (10) we can now find the coefficients $(-1)^{J+1} F^{4\ J\ J}_{A_1\ p\ p}$ to second order of approximation. From Eq. (7) we see that these coefficients are just the energies T_{JM} divided by $-(J \| 4 \| J)$. Thus along the fourfold axes the center of gravity of $(-1)^{J+1} F^{4\ J\ J}_{A_1\ p\ p}$ corresponding to the states $|\begin{smallmatrix} p \\ a \end{smallmatrix} JM)$ in Eq. (11) is given by

$$H_{JM} = -T_{JM}/(J \| 4 \| J) = H^1_{JM} + H^2_{JM}, \quad (12)$$

where

$$H^1_{JM} = (-1)^{J-M+1} \sqrt{\frac{7}{12}} \begin{pmatrix} J & 4 & J \\ -M & 0 & M \end{pmatrix}, \quad (13a)$$

$$H^2_{JM} = \sqrt{\frac{5}{24}} \left\{ \frac{\begin{pmatrix} J & 4 & J \\ -(M+4) & 4 & M \end{pmatrix}^2}{H^1_{JM} - H^1_{JM+4}} + \frac{\begin{pmatrix} J & 4 & J \\ -(M-4) & -4 & M \end{pmatrix}^2}{H^1_{JM} - H^1_{JM-4}} \right\}. \quad (13b)$$

Similarly, along the threefold axes we find

$$H^1_{JM} = (-1)^{J-M} \frac{2}{3} \sqrt{\frac{7}{12}} \begin{pmatrix} J & 4 & J \\ -M & 0 & M \end{pmatrix}, \quad (14a)$$

TABLE I. The first and second order approximate expressions for the cluster center of gravity of $(-1)^{J+1}F^{4JJ}_{A_1pp}$ along the fourfold and threefold axes are compared with their actual value H for $J=30$ to $J=5$.

	Fourfold axes			Threefold axes		
	H^1_{JJ}	$H^1_{JJ}+H^2_{JJ}$	H	H^1_{JJ}	$H^1_{JJ}+H^2_{JJ}$	H
$J=30$	−0.082991526	−0.082995600	−0.082995607	0.055328	0.055707	0.055738
$J=29$	−0.083917495	−0.083922114	−0.083922122	0.055945	0.056359	0.056394
$J=28$	−0.084869295	−0.084874557	−0.084874568	0.056580	0.057033	0.057073
$J=27$	−0.085847407	−0.085853432	−0.085853446	0.057232	0.057729	0.057776
$J=26$	−0.086852155	−0.086859091	−0.086859109	0.057901	0.058449	0.058504
$J=25$	−0.087883646	−0.087891680	−0.087891704	0.058589	0.059195	0.059259
$J=24$	−0.088941691	−0.088951058	−0.088951089	0.059294	0.059967	0.060044
$J=23$	−0.090025690	−0.090036689	−0.090036732	0.060017	0.060768	0.060858
$J=22$	−0.091134492	−0.091147511	−0.091147568	0.06076	0.06160	0.06171
$J=21$	−0.092266193	−0.092281738	−0.092281818	0.06151	0.06246	0.06259
$J=20$	−0.09341787	−0.09343661	−0.09343672	0.06228	0.06336	0.06351
$J=19$	−0.09458521	−0.09460805	−0.09460821	0.06306	0.06429	0.06447
$J=18$	−0.09576200	−0.09579018	−0.09579043	0.06384	0.06526	0.06547
$J=17$	−0.09693942	−0.09697467	−0.09697506	0.06463	0.06628	0.06652
$J=16$	−0.09810504	−0.09814984	−0.09815045	0.06540	0.06734	0.06762
$J=15$	−0.0992413	−0.0992993	−0.0993003	0.06616	0.06847	0.06875
$J=14$	−0.1003237	−0.1004004	−0.1004021	0.06688	0.06966	0.06992
$J=13$	−0.1013172	−0.1014214	−0.1014240	0.06754	0.07094	0.07119
$J=12$	−0.1021721	−0.1023181	−0.1023219	0.06811	0.07235	0.07231
$J=11$	−0.1028166	−0.1030292[a]	−0.1030333	0.06854	0.07394[b]	0.07339
$J=10$	−0.1031455	−0.1034711[a]	−0.1034668	0.0688	0.0759[b]	0.0748
$J=9$	−0.103002	−0.103535[a]	−0.103487	0.0687	0.0783[b]	0.0748
$J=8$	−0.10215	−0.10311[a]	−0.10291	0.0681	0.0820[b]	0.0741
$J=7$	−0.10022	−0.10222[a]	−0.10141	0.0668	0.0884[b]	0.0748
$J=6$	−0.0966	−0.1021[a]	−0.0976	0.0644	0.1023[b]	0.0652
$J=5$	−0.0903	−0.1226[a]	−0.0892	0.0602	0.1462[b]	0.0443

[a]No cluster for $m=J-4$.
[b]No cluster for $m=J-3$.

$$H^2_{JM}=\frac{16}{9}\sqrt{\frac{5}{24}}\left\{\frac{\begin{pmatrix} J & 4 & J\\ -(M+3) & 3 & M\end{pmatrix}^2}{H^1_{JM}-H^1_{JM+3}}+\frac{\begin{pmatrix} J & 4 & J\\ -(M-3 & -3 & M\end{pmatrix}^2}{H^1_{JM}-H^1_{JM-3}}\right\}. \tag{14b}$$

In Table I we calculate H^1_{JJ} and H_{JJ} along the four- and threefold axes for $J=30$ to $J=5$ and compare them with the correct center of gravities of the clusters found by Krohn[12] by actually diagonalizing T_{A_1}. We see that the H_{JJ} are accurate even for $J<20$. The maximum value of H_{JM} occurs when $|{}^J_M\rangle$ is directed along the threefold axes and when $J=M$. The minimum value of H_{JM} occurs when $|{}^J_M\rangle$ is directed along the fourfold axes and when $J=M$. From Eq. (1) we see that the H_{JJ} along the three- and fourfold axes in Table I give the upper and lower cluster energies and thus delineate the limbs of the cluster spectra. Notice that for high J where $H^2_{JM}\ll H^1_{JM}$ the splitting ratio of the upper (threefold axes) cluster energy to the lower (fourfold axes) cluster energy within a J manifold is $-\frac{2}{3}$.[13]

To determine all the cluster energies for a given J we calculate the H_{JM} along the threefold axes (high energy) and fourfold axes (low energy) for $M=J, J-1, \ldots$ as in Table II where $J=30$. Notice that the accuracy of our approximation decreases with decreasing M. For low M where $H^1_{JM}\sim H^2_{JM}$ our perturbative approach becomes invalid, but fortunately this occurs near where the clusters arising from the threefold axes cross with those arising from the fourfold axes. As noted by Dorney and Watson,[14] this crossing occurs near the H_{JJ} for the twofold octahedral axes where

$$T_{A_1}=-\tfrac{1}{4}\left[\sqrt{\tfrac{7}{12}}\,V^4_0-\sqrt{\tfrac{35}{8}}\,(V^4_2+V^4_{-2})-\sqrt{\tfrac{15}{8}}\,(V^4_4+V^4_{-4})\right]. \tag{15}$$

Thus for high J the crossing occurs at an energy of $-\frac{1}{4}$, the lowest cluster energy.

In Fig. 1 we compare our cluster spectra derived from Table II with the spectra resulting from actually diagonalizing T_{A_1} for $J=30$. Note that the cluster for $M=28$ along the threefold axes have nearly the same energy as the cluster for $M=24$ along the fourfold axes. Thus we may consider the O_h terms at this crossing as arising from a cluster T_1+E+T_2 of 1_3 or from a cluster A_1+T_1+E of O_4. In both cases the error of the approximate center of gravity is less than 10%.

If one needs to calculate contributions to the centrifugal distortion of sixth order in J, the symmetry-adapted vector coupling coefficients $F^{4\,J\,J}_{A_1\,p\,p}$ can be approximated in a similar manner. Here one needs the sixth rank octahedral scalar

$$T_{A_1}=\tfrac{1}{8}\left[V^6_0-\sqrt{\tfrac{7}{2}}\,(V^6_4+V^6_{-4})\right], \tag{16a}$$

along the fourfold axes or

TABLE II. The first and second order approximate expressions for the cluster center of gravity of $(-1)^{J+1}F^4_{A_1}{}^{J}_{p}{}^{J}_{p}$ along the fourfold and threefold axes are compared with their actual value H for $J=30$ and different M.

	Fourfold axes			Threefold axes		
$J=30$	H^1_{JM}	$H^1_{JM}+H^2_{JM}$	H	H^1_{JM}	$H^1_{JM}+H^2_{JM}$	H
$M=30$	−0.082991526	−0.082995600	−0.082995607	0.055328	0.055707	0.055738
$M=29$	−0.05532768	−0.05535064	−0.05535074	0.03689	0.03849	0.03877
$M=28$	−0.03188375	−0.03196295	−0.03196377	0.02126	0.02558	0.02632
$M=27$	−0.0123202	−0.0125387	−0.0125444	0.00821	0.01735	0.01443
$M=26$	0.003691	0.003157	0.003123	−0.00246	0.01479	−0.00280
$M=25$	0.01646	0.01522	0.01511	−0.0110	−0.0153	−0.0247
$M=24$	0.02630	0.02332	0.02434	−0.018	−0.027	−0.056
$M=23$	0.03350	0.03372	0.03331	−0.022	−0.041	−0.083
$M=22$	0.0383	0.0388	0.0419			
$M=21$	0.041	0.042	0.056			
$M=20$	0.042	0.042	0.056			

$$T_{A_1}=\tfrac{1}{8}\left[\tfrac{16}{9}V^6_0+\tfrac{2}{9}\sqrt{70}\,(V^6_3-V^6_{-3})+\tfrac{2}{9}\sqrt{77}\,(V^6_6+V^6_{-6})\right] \quad (16b)$$

along the threefold axes. For high J the splitting ratio of the upper cluster energy to the lower cluster energy within a J-manifold is now $\frac{16}{9}$.

For $J>30$ one may use the approximate expression for the 3-j coefficients given by Edmonds[15]

$$(-1)^{J-M}\begin{pmatrix} J & K & J \\ -M & 0 & M \end{pmatrix}=P_K(\cos\theta);\ K \text{ even} \quad (17)$$

where

$$\cos\theta=M/[J(J+1)]^{1/2}$$

to estimate the cluster energies Eq. (13a) and (14a). The P_K are the Legendre polynomials. For $K=4$ the error introduced when $M=J=30$ is about 0.6% and when $M=J=100$ about 0.05%. In Table III we give the approximate cluster energies along the four- and threefold axes using Eq. (17) and compare them with the actual values found by Krohn for $J=100$. Equation (17) is convenient because computer calculations of the 3-j coefficients for $J>30$ can lead to overflow problems.

SPLITTING OF CLUSTERS

The splitting of the degenerate basis $|{}^{p}_{a}JM\rangle$ in Eq. (11) is found by diagonalizing our potential T_{A_1} in a basis directed along the different four- or threefold

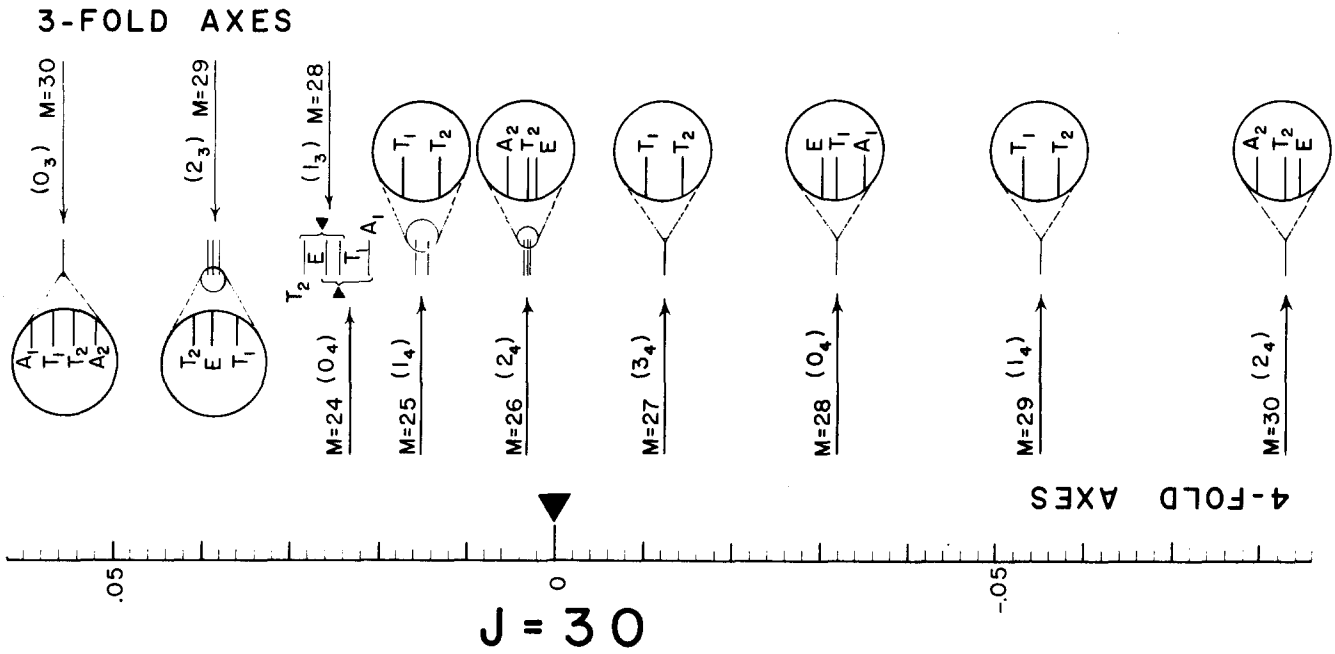

FIG. 1. Cluster spectra of SF_6 for $J=30$. The approximate cluster energies for the threefold axes (right arrows) and fourfold axes (left arrows) are compared with the spectra found by diagonalization of the octahedral deformation potential for $J=30$. The approximate cluster energies are accurate to within the resolution shown for upper and lower clusters. At the crossing over of clusters the labeling is ambiguous and the arrows differ from the center of gravity of the clusters as indicated. Note that the splitting ratio of the upper cluster to the lower cluster is $-\frac{2}{3}$. The splitting ratios within each cluster as shown within the circles is as predicted in Article I.

TABLE III. An asymptotic expression for the 3-j coefficients is used to evaluate the first order approximate cluster center of gravity H^1_{JM} and compared with their actual value H for $J=100$.

	Fourfold axes		Threefold axes	
$J=100$	$\sim H^1_{JM}$	H	$\sim H^1_{JM}$	H
$M=100$	−0.051228	−0.051256	0.034152	0.034189
$M=99$	−0.046104	−0.046131	0.030736	0.030829
$M=98$	−0.041212	−0.041238	0.02747	0.02768
$M=97$	−0.036546	−0.036571	0.02436	0.02476
$M=96$	−0.032102	−0.032127	0.02140	0.02206
$M=95$	−0.027872	−0.027899	0.0186	0.0196
$M=94$	−0.023853	−0.023884	0.0159	0.0174
$M=93$	−0.020039	−0.020075	0.0134	0.0155
$M=92$	−0.016425	−0.016469	0.0110	0.0139[a]
$M=91$	−0.013005	−0.013062	0.0087	0.0125
$M=90$	−0.009775	−0.009849	0.0065	0.0107
$M=89$	−0.006730	−0.006825		
$M=88$	−0.00386	−0.00399		
$M=87$	−0.00117	−0.00133		
$M=86$	0.00134	0.00114		
$M=85$	0.00371	0.00343		
$M=84$	0.00590	0.00555		
$M=83$	0.00794	0.00748		
$M=82$	0.00983	0.00923		
$M=81$	0.01157	0.01078		
$M=80$	0.0131	0.0121		
$M=79$	0.0146	0.0133[a]		
$M=78$	0.0160	0.0143		
$M=77$	0.0172	0.0155		

[a]Crossover.

axes. We thus form a six or eight dimensional representation of O_h with matrix elements given by the axis tunneling amplitudes S, T, U, ... between nearest axes, next to nearest axes, etc. In Article (I) we have shown that for states $|{}^p_a JM\rangle$ directed along the fourfold axes we have the following cluster splittings for IR M_4 of C_4:

O_4	1_4	2_4	3_4
A_1: $H+4S+T$	T_2: $H+2S$	E: $H+2S+T$	T_2: $H+2S$
T_1: $H-T$	T_1: $H-2S$	T_2: $H-T$	T_1: $H-2S$
		E: $H-2S+T$	A_2: $H-4S+T$

(18a)

Similarly, for states $|{}^p_a JM\rangle$ directed along the threefold axes we have the following cluster splittings for IR M_3 of C_3:

O_3	1_3	2_3
A_1: $H+3S+3T+U$	T_2: $H+2S-T$	T_2: $H+2S-T$
T_1: $H+S-T-U$	E: $H+3T$	E: $H+3T$
T_2: $H-S-T+U$	T_1: $H-2S-T$	T_1: $H-2S-T$
A_2: $H-3S+3T-U$		

(18b)

Note that the center of gravity of each cluster H is preserved under the splittings. We have shown in the previous section that the center of gravity of a cluster to second order of approximation H_{JM} is easy to calculate and is surprisingly accurate even for $J<20$. We now proceed to calculate the nearest neighbor tunneling amplitudes for the four- and threefold axes.

Let the operator $O_R(\alpha,\beta,\gamma)$ rotate state $|{}^p_a JM\rangle$ by Euler angles such that

$$O_R(\alpha,\beta,\gamma)\left|{}^J_M\right\rangle = \sum_{M'} e^{-iM'\alpha} d^J_{M'M}(\beta)\, e^{-iM\gamma}\left|{}^J_{M'}\right\rangle, \tag{19}$$

where the $d^J_{M'M}(\beta)$ are the standard angular momentum representations for finite rotations (β).[16] We wish to find the Euler angles such that the operators $O_R(\alpha,\beta,\gamma)$ transform states $|{}^p_a JM\rangle$ between nearest neighbor four- or threefold axes. These operators will then be equivalent to certain coset leaders of C_4 or C_3 that have already been given in Article I. For example, the operator corresponding to coset leader i_1 of C_4 is $O_R(0,\ 90°,\ \pi)$ and the operator corresponding to coset leader i_1 of C_3 is $O_R(0,\ \cos^{-1}\frac{1}{3},\ \pi)$.

Let us consider the tunneling amplitude $\langle{}^p_a JM|\, T_{A_1}\, O_R(0,\ 90°,\ \pi)\,|{}^p_a JM\rangle$ between fourfold axes for $J<12$. Since there does not exist any cluster for $|{}^J_{M'}\rangle = |{}^J_{M\pm4}\rangle$ when $J<12$, we see from Eq. (11) that $|{}^p_a JM\rangle = |{}^J_M\rangle$, and

$$\left\langle {}^p_a JM\right| T_{A_1} O_R(0,\ 90°,\ \pi)\left|{}^p_a JM\right\rangle = \sqrt{\frac{7}{12}}\left\langle {}^J_M\right| V^4_0 \left|{}^J_M\right\rangle d^J_{MM}(90°)(-1)^M + \sqrt{\frac{5}{24}}\left\langle {}^J_M\right| V^4_4 \left|{}^J_{M-4}\right\rangle d^J_{M-4\,M}(90°)(-1)^M. \tag{20}$$

The first term on the right may be shown to be the correction due to the nonorthogonality of our basis. Dividing the remaining term by $-(J\|4\|J)$ we find the tunneling amplitude corresponding to $(-1)^{J+1}F^{4\ J\ J}_{A_1\ p\ p}$ for the fourfold axes to be

$$S_{JM} = (-1)^{J+1}\sqrt{\frac{5}{24}}\begin{pmatrix} J & 4 & J \\ -M & 4 & M-4\end{pmatrix} d^J_{M-4\,M}(90°). \tag{21}$$

Using Eq. (21) for $J=8$, we find the following tunneling amplitudes:

$J=8$	S_{JM}	S
$M=8$	−0.001995	−0.001825
$M=7$	−0.008979	−0.009965 .

(22)

Naturally, as J and M decrease, our states $|{}^J_M\rangle$ become less accurate as do the corresponding S_{JM}.

When $J\geq12$ we have to consider the higher order terms for $|{}^p_a JM\rangle$ in Eq. (11). The dominant terms for S_{JM} are

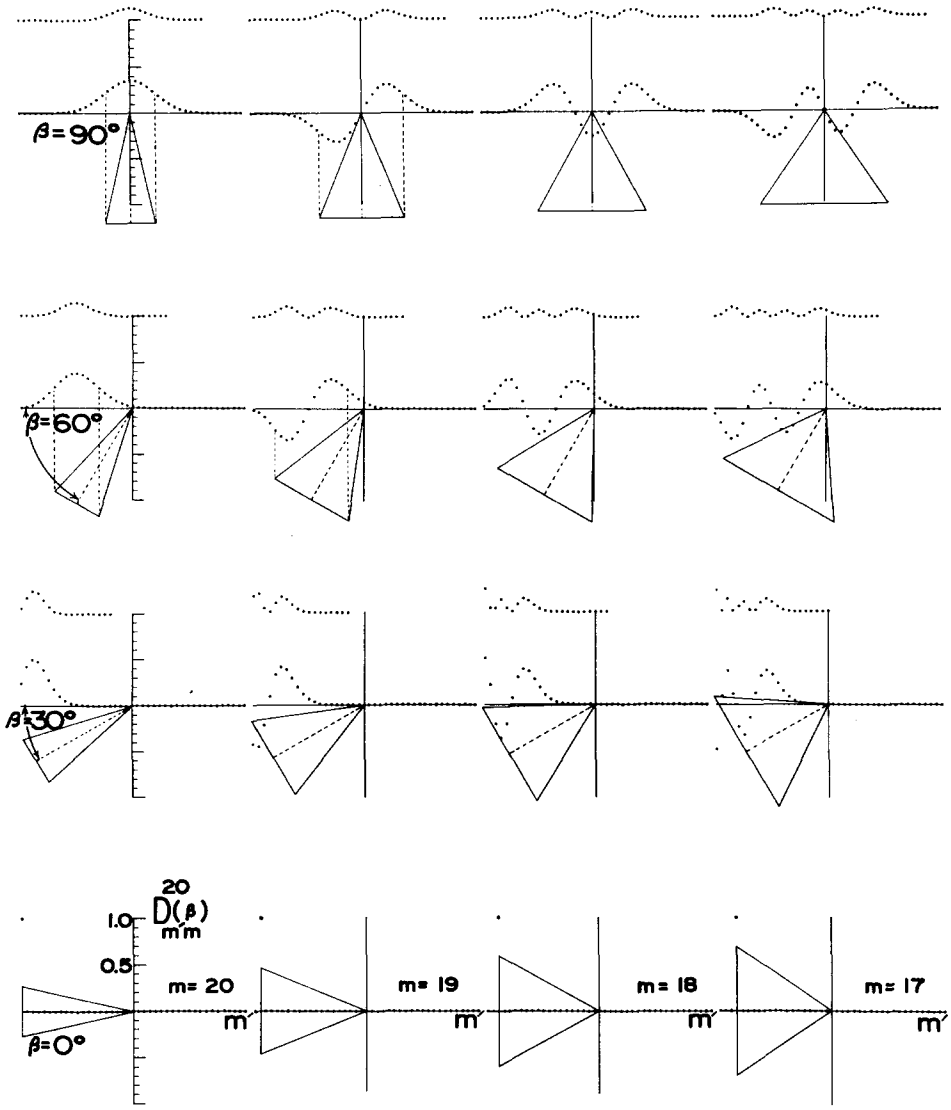

FIG. 2. Behavior of rotation matrix elements. The rotation matrix elements $d^{20}_{m'm}(\beta)$ and their squares are plotted for various angles β and m against m' (decreasing to the right). The inflection points for the exponential tails in these plots are determined by using angular momentum cones. The cones have a height of length m and sides of length $\sqrt{J(J+1)}$ and are rotated β degrees counterclockwise from the m' axis.

$$S_{JM} = (-1)^{J+1}\sqrt{\frac{5}{24}}\begin{pmatrix} J & 4 & J \\ -M & 4 & M-4 \end{pmatrix} d^J_{M-4\,M}(90°) + \sigma\begin{pmatrix} J & 4 & J \\ -(M-4) & 4 & M-8 \end{pmatrix} d^J_{M-8\,M}(90°) + \cdots \Big], \quad (23)$$

where

$$\sigma = (-1)^{J-M+1}\sqrt{\frac{5}{24}}\frac{\begin{bmatrix} J & 4 & J \\ -(M-4) & -4 & M \end{bmatrix}}{H^1_{JM} - H^1_{JM-4}} .$$

The second term in Eq. (23) arises from the mixing of state $|{}^J_{M-4}\rangle$ into $|{}^p_a\, JM\rangle$. Higher order terms in Eq. (23) occur when $J \geq 24$ and arise from the mixing of states $|{}^J_{M-8}\rangle$, $|{}^J_{M-12}\rangle$, ... into $|{}^p_a\, JM\rangle$. Although for large J and M the mixing coefficients σ are small, the contribution to the tunneling from state $|{}^J_{M-4}\rangle$ is much greater than the contribution from state $|{}^J_M\rangle$ so that the terms in Eq. (23) are *increasing* in magnitude. However, these terms become more inaccurate because the states $|{}^J_{M-4}\rangle$, $|{}^J_{M-8}\rangle$, ... become less accurate approximations for the cluster states. Thus it is impossible to calculate S_{JM} for high M any more accurately than S_{JM} for low M. Furthermore, calculations for high J and M become more and more tedious since more terms in Eq. (23) must be evaluated. However, Eq. (23) can still be useful for order of magnitude calculations.

Even more useful is the fact that we can use Eq. (23) to derive the sign for S_{JM} and thus the ordering of terms within each cluster. Analysis of the terms in Eq. (23) reveals each to have a sign $(-1)^{J-M+1}$ so that for the fourfold axes

$$\text{sgn } S_{JM} = (-1)^{J+1}. \quad (24)$$

Calculations of S by actually diagonalizing T_{A_1} have revealed this sign law to be valid and $T<S<H$ for *all* fourfold clusters with $J=1$ to $J=100$. Because of this we find the following ordering for increasing energy within *any* J manifold,

$$\begin{array}{lcccccccc} J \text{ even:} & \underbrace{A_1\ T_1\ E}_{0_4} & & \underbrace{T_2\ T_1}_{3_4} & & \underbrace{E\ T_2\ A_2}_{2_4} & & \underbrace{T_2\ T_1}_{1_4} & \\ J \text{ odd:} & \underbrace{E\ T_1\ A_1}_{0_4} & & \underbrace{T_1\ T_2}_{3_4} & & \underbrace{A_2\ T_2\ E}_{2_4} & & \underbrace{T_1\ T_2}_{1_4} & . \end{array} \quad (25)$$

This ordering is in agreement with experiment.[17] As an example, for increasing energy we have terms $E\ T_2$ for $J=2$ and terms $T_1\ T_2$, $E\ T_1\ A_1$, $T_1\ T_2$, A_2 for $J=9$.

Note that this provides a convenient way to decompose any J into IR of T_d or O_h (ignoring parity) since one needs only to remember the terms in two clusters and their proper ordering for a given J.

The equation for the tunneling amplitude for the threefold axes corresponding to Eq. (23) is

$$S_{JM} = (-1)^{J+1} \frac{4}{3} \sqrt{\frac{5}{24}} \left[\begin{pmatrix} J & 4 & J \\ -M & 3 & M-3 \end{pmatrix} d^J_{M-3\,M}(71^\circ) - \sigma \begin{pmatrix} J & 4 & J \\ -(M-3) & 3 & M-6 \end{pmatrix} d^J_{M-6\,M}(71^\circ) + \cdots \right], \quad (26)$$

where

$$\sigma = (-1)^{J-M+1} \frac{4}{3} \sqrt{\frac{5}{24}} \frac{\begin{pmatrix} J & 4 & J \\ -(M-3) & -3 & M \end{pmatrix}}{H^1_{JM} - H^1_{J\,M-3}} .$$

Analysis of the terms in Eq. (26) reveals each to have a sign $(-1)^J$ so that for the threefold axes

$$\operatorname{sgn} S_{JM} = (-1)^J. \quad (27)$$

Again, this sign law is valid and F, $T < S < H$ for *all* threefold clusters within a J manifold and for *all* J. Thus we have the following ordering for decreasing energy with *any* J manifold:

$$\begin{array}{lccccc} J \text{ even:} & \underbrace{A_1\ T_1\ T_2\ A_2} & & \underbrace{T_2\ E\ T_1} & & \underbrace{T_2\ E\ T_1} \\ & O_3 & & 2_3 & & 1_3 \\ J \text{ odd:} & \underbrace{A_2\ T_2\ T_1\ A_1} & & \underbrace{T_1\ E\ T_2} & & \underbrace{T_1\ E\ T_2} \end{array} . \quad (28)$$

For decreasing energy we have terms T_2 E for $J = 2$ and terms A_2 T_2 T_1 A_1, T_1 E T_2, T_1 for $J = 9$ as before. Again, we need only remember the terms in two clusters and their proper ordering to decompose any J into IR of T_d or O_h. Note that Eqs. (25) and (28) verify Fig. 7 of Article I.

We have already noted (see Fig. 1) that the crossing of the three- and fourfold clusters occurs closer to the upper limb than the lower; that is, the clusters along the fourfold axes do not split as much as along the threefold axes and continue to be valid (U, $T < S < H$) for lower M. The tunneling amplitude S for the fourfold axes is much smaller than for the threefold axes for a given M because the interaxial angle is larger ($90^\circ > 71^\circ$) and the rotation matrix elements $d^J_{M'M}(\beta)$ are smaller. In Fig. 2 we show the general behavior of the $d^J_{M'M}(\beta)$ for which M' and M are left of the left inflection points in the figure. Note that for these M' and M, $d^J_{M'M}(\beta)$ increases with decreasing angle (β). For a given M and angle (β), $d^J_{M'M}(\beta)$ increases with decreasing M' and for a given M' and angle (β), $d^J_{M'M}(\beta)$ increases with decreasing M. Furthermore, since we are in the exponential region left of the left inflection point, the sign of $d^J_{M'M}(\beta)$ may be readily evaluated.

ACKNOWLEDGMENT

We sincerely thank Dr. Burt Krohn of Los Alamos Laboratories who provided us with the computer output for calculations of the symmetry adapted vector coupling coefficients for $J = 1$ to $J = 100$.

[1] J. P. Aldridge *et al.*, J. Mol. Spectrosc. 58, 165 (1975).
[2] R. S. McDowell *et al.*, Optics Commun. 17, 178 (1976).
[3] K. T. Hecht, J. Mol. Spectrosc. 5, 355 (1960).
[4] J. Moret-Bailly, J. Mol. Spectrosc. 15, 344 (1965).
[5] K. Fox (private communication).
[6] J. Moret-Bailly, J. Mol. Spectrosc. 15, 355 (1965).
[7] K. Fox and I. Ozier, J. Chem. Phys. 52, 5044 (1970).
[8] Moret-Bailly, J. Phys. (Paris) 36, 451 (1975).
[9] A. J. Dorney and J. K. G. Watson, J. Mol. Spectrosc. 42, 135 (1972).
[10] W. G. Harter and C. W. Patterson, J. Chem. Phys. 66, 4872 (1977), preceding article.
[11] Reference 8.
[12] B. Krohn (private communication).
[13] This has been shown in Ref. 9 using a classical argument.
[14] Reference 9.
[15] A. R. Edmonds, *Angular Momentum in Quantum Mechanics* (Princeton Univ., Princeton, 1957), p. 122.
[16] For the definition of the Euler angles and the rotation matrices we are using see M. Tinkham, *Group Theory and Quantum Mechanics* (McGraw-Hill, New York, 1964).
[17] References 1 and 2.